Journal of Advanced Marine Engineering and Technology, Vol. 46, No. 6, pp. 342~347, 2022
J. Advanced Marine Engineering and Technology (JAMET)
https://doi.org/10.5916/jamet.2022.46.6.342

ISSN 2234-7925 (Print)
ISSN 2765-4796 (Online)
Original Paper

Understanding of microstructures and mechanical properties of thermal sprayed Ni-based coatings with Al and Mo addition

Jaehui Bang[1] · Hansol Kwon[2] · Eungsun Byon[3] · Eunkyung Lee[†]

(Received December 7, 2022 ; Revised December 19, 2022 ; Accepted December 26, 2022)

Abstract: In this study, the mechanical properties of Ni coating implemented with twin wire arc spray (TWAS) were analyzed by adding Al and Mo to improve the surface properties of high-strength low-alloy steel. The effect of the additive element on the nickel coating was suggested through microstructure analysis such as grain size and intermetallic compounds, and the applicability of Mo in the Ni-Al coating was evaluated. In the Ni-5Al coating, when the Al content was increased to 20Al, the grain size decreased by 19.81%, and when Mo was added, it decreased by 8.91% in Ni-5.5Al-5Mo. In addition, the more Al was added, the more intermetallic compounds of NiAl and Ni_3Al formed. This is because the increase in Al content and the addition of Mo caused FCC lattice structure expansion and provided the driving force for solid solution formation. As a result of the microhardness test, the mechanical properties of Ni-20Al and Ni-5.5Al-Mo increased by 121.68% and 16.58%, respectively, compared to Ni-5Al.

Keywords: Twin wire arc spray, Coating, Ni-5Al, Ni-20Al, Ni-5.5Al-5Mo, Microstructure, Mechanical Property

1. Introduction

High-strength low-alloy (HSLA) steels, which have better mechanical properties than conventional steel, require high durability (or lifespan) because they are used not only for marine structures but also for high-temperature environments of boilers and turbine engines of ships **[1]-[3]**. The most effective way to improve the surface characteristics of steel is surface coating using a coating material that will enhance the corrosion resistance and mechanical properties of metal and has excellent properties and oxidation resistance even at high temperatures **[4]-[7]**. Thermal spray methods such as flame spray, high velocity oxygen fuel (HVOF), plasma arc spray (PAS), and wire arc spray (WAS) are mainly used for surface protection. Among them, wire arc spray technologies are used in many surface and repair industries owing to their characteristics, namely their low cost, high spraying rate, and high deposition efficiency **[8]-[11]**.

Chromium (Cr), Nickel (Ni), Aluminum (Al), Molybdenum (Mo), etc. are used as materials for surface coating **[12]**, and Ni is used in various applications that require high temperature and corrosion protection because it can improve the resistance of metals and is resistant to wear and heat **[13]-[14]**. Al added to improve the castability of Ni coating is often used in extreme environments requiring chemical and mechanical stability at high temperatures and corrosion resistance, and it is dissolved in Ni to form a solid solution **[11]-[12]**, **[15]**. The addition of Al in Ni coating can increase the binding force between the substrate and top coating by an adjunct alumina scale and prevent the delamination phenomenon in the coating layer or between the coating layer and substrate **[15]**. In addition, Ni-Al intermetallic compounds produced by the chemical reactions of each element are widely used in the coating industry for their high resistance to high temperature oxidation and good mechanical properties.

† Corresponding Author (ORCID: http://orcid.org/0000-0003-0723-8524): Associate Professor, Interdisciplinary Major of Maritime AI Convergence, Department of Ocean Advanced Materials Convergence Engineering, Korea Maritime & Ocean University, 727, Taejong-ro, Yeongdo-gu, Busan 49112, Korea, E-mail: elee@kmou.ac.kr, Tel: 051-410-4353

1 M. S. Candidate, Interdisciplinary Major of Maritime AI Convergence, Department of Ocean Advanced Materials Convergence Engineering, Korea Maritime & Ocean University, E-mail: J.Bang@g.kmou.ac.kr, Tel: 051-410-4955

2 Ph. D., Surface Materials Division, Department of Extreme Environmental Coatings, Korea Institute of Materials Science, E-mail: hskwon@kims.re.kr, Tel: 055-280-3645

3 Ph. D., Surface Materials Division, Department of Extreme Environmental Coatings, Korea Institute of Materials Science, E-mail: esbyon@kims.re.kr, Tel: 055-280-3555

Table 1: Process parameter of twin wire arc spray, TWAC process parameters used to spray coating

Spray Parameters	Unit		
Coating materials	Ni-5Al	Ni-5.5Al-5Mo	Ni-20Al
Wire diameter	1.6 mm	1.6 mm	1.6 mm
Voltage	36 V	36 V	36 V
Current	250 A	250 A	200 A
Air pressure	70 psi	70 psi	70 psi
Spray Distance	200 mm	200 mm	200 mm
Thickness	1000 μm	1500 μm	1000 μm
Gun spraying angle	90	90	90

Owing to its low density and good electrical and thermal conductivity, it is used in a wide range of engineering applications **[11] [14]**.

Kornienko. E, *et al.* coated Ni75Al25 using atmospheric plasma spraying (APS) and high-velocity plasma spraying (HV-APS) methods and then compared the characteristics of the coatings according to the coating process. It was proved that HV-APS coating has excellent oxidation resistance at high temperatures by reducing porosity compared to APS coating **[16]**. Hamed. K et al, who analyzed the microstructure of plasma sprayed Ni-Al coating in AISI 304 stainless steel, studied the microstructure and mechanical properties that change according to the amount of mixed Al, Ni/Al, and Ni5Al powders. The mechanical properties based on the increment of the Ni-based percentage in the coating mixture were analyzed, and this was verified with the intermetallic compound **[17]**. Mihailo R. Mrdak found the optimal process variable in the APS process by analyzing the mechanical properties and microstructure based on process parameters in the coating process of atmospheric plasma spray (APS) coatings of Ni5.5wt.%Al5wt.%Mo **[18]**. Although many studies have been conducted on the microstructure analysis and mechanical evaluation of Ni-Al and Ni-Mo coatings, studies focusing on the Al content are insufficient, and more attention is needed on the change in mechanical properties due to the addition of Mo in Ni-Al coatings.

This study analyzed the change in the mechanical characteristics of Ni-based coating due to the addition of Al content and Mo coated with the Twin Wire Arc Spray process to protect Fe-3.5Ni-1.29Cu alloy. In addition, the characteristic change according to each element's content is explained from a microstructural perspective for comparative analysis and to evaluate the applicability of Mo in Ni-Al coatings.

2. Experimental materials and methods

2.1 Twin wire arc spray

Fe-3.5Ni-1.29Cu alloy (HSLA-100), a high-strength low alloy (HSLA) steel, was used as the substrate sample. Its chemical composition was 3.5% Ni, 1.29% Cu, 0.5% Mn, 0.209% Si, 0.048 C, 0.037% Nb, 0.003% V, 0.025% Al, 0.002% S, 0.008% P, and Fe to balance. All substrates were subjected to Ni-based coating after roughening using Alumina Grit blasting to improve the bonding strength of the substrate and coating layer for 2 passes at a grit size of 20 mesh, air pressure of 6 bar, and distance of 200 mm. Twin Arc Spray Coating was performed under the process conditions listed in **Table 1** using Auto Arc AVD HD 456 (Thermion, USA) equipment for three types of wire: Ni-5Al solid wires, Ni-20Al cored wires, and Ni-5.5Al-5Mo cored wires.

2.2 Microstructure and microhardness test of Ni-based coatings

For microstructure analysis of the coating layer and the substrate, polishing was performed using a SiC polishing cloth from 200 to 2400 grit and using 9 μm, 3 μm, and 1 μm diamond suspension and 0.04 μm colloidal. The characteristics of the coated layer and substrate were observed using a field emission scanning electron microscope (FE-SEM; MIRA3, TESCAN, accelerating voltage: 10.0 kV) and energy dispersive spectrometer (EDS, EDAX). Image analysis was conducted to measure the porosity and oxide area fraction of the deposited layers. To analyze the crystal with the addition of Al and Mo, x-ray diffraction (XRD; Rigaku, D/MAX 2500 V L/PC, 40 kv, 30 mAh) using Cu Kα radiation (λ =1.54 Å) was performed. Electron backscatter diffraction (EBSD; TESCAN CLARA, Oxford Nordlys Nano, accelerating voltage: 20.0 kV, current: 10 nA, step size: 1 μm) and ATEX-software were also used to analyze the grain size of the coating layers. A High-Resolution 3D Microscope (KEYENCE, VHX-7000) was used to measure the surface roughness of each

coating layer. The Ra value was an average of three positions of two readings. The hardness distribution was observed at intervals of 0.1 mm from a point 1 mm from the top surface, according to the ASTM E384 standard, and the load was set to 0.1 kgf load for 10 s using the Micro Vickers hardness test with an HM-122 hardness test machine (Akashi Co., Tokyo, Japan).

3. Results and discussion

3.1. Surface roughness

Figure 1 shows the analysis of the surface roughness of the coated sample on which the twin wire arc spray coating process parameters listed in **Table 1** were applied with a High-Resolution 3D Microscope. It can be seen that the surface roughness changed according to the Al content of the Ni based coating and the addition of Mo. Ni-5Al, Ni-20Al, and Ni-5.5Al-5Mo have surface roughness of 13.6375 (±1.21) Ra, 10.8625 (±1.11) Ra, and 11.0125 (±1.05) Ra, respectively. When the molten coating material at the high temperature of the process cools before it comes into close contact with the substrate and exists as an unmelted part, a rough surface occurs, and it changes depending on the twin wire arc spray process parameters such as feed speed and coating voltage **[14]**. Particles that are not completely melted during the deposition process are solid, so they are coated while maintaining their original shape, resulting in a rough surface. That is, it is coated while minimizing shape change.

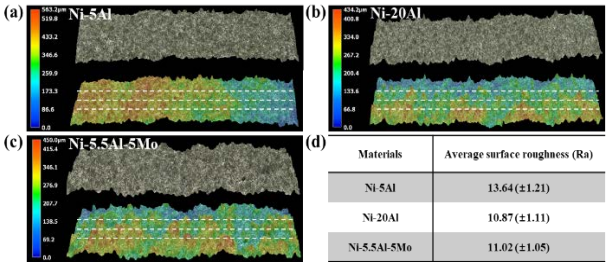

Materials	Average surface roughness (Ra)
Ni-5Al	13.64 (±1.21)
Ni-20Al	10.87 (±1.11)
Ni-5.5Al-5Mo	11.02 (±1.05)

Figure 1: Surface roughness images of (a) Ni-5Al, (b) Ni-20Al, (c) Ni-5.5Al-5Mo coated layers and values of the coating materials

3.2 Microstructure of coating layers

The secondary electron (SE) images of the cross-section of the sprayed sample are shown in **Figure 2**. As shown in **Figure 2**, a typical microstructure of arc sprayed coating can be seen, with a continuous deposited layer of splat caused by molten particles colliding with the substrate and the lamellar structure, including porosity, crack, and oxides found on the split boundaries. The

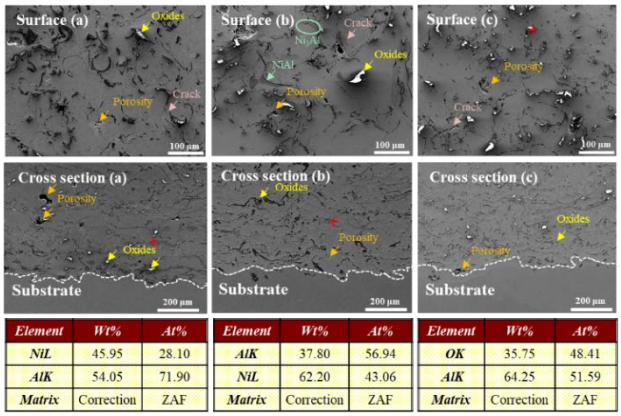

Element	Wt%	At%
NiL	45.95	28.10
AlK	54.05	71.90
Matrix	Correction	ZAF

Element	Wt%	At%
AlK	37.80	56.94
NiL	62.20	43.06
Matrix	Correction	ZAF

Element	Wt%	At%
OK	35.75	48.41
AlK	64.25	51.59
Matrix	Correction	ZAF

Figure 2: Microstructure of **the** surface and cross section of (a) Ni-5Al, (b) Ni-20Al and (c) Ni-5.5Al-5Mo and EDS results at the red cross markers

lamellar structure is also formed when the coating material particles are not completely melted or melted before reaching the substrate but are re-solidified or unmixed with oxides formed by their reaction with oxygen in the atmosphere.

The black parts in (a) and (b) of **Figure 2** are porosity, cracks, and oxides caused by a failure to completely melt between the split and another split **[8]**, and the gray parts are NiAl intermetallic phase, the light gray parts are the Ni_3Al intermetallic compounds, and the white parts are cracks and oxides. The red cross markers of A(b) and C(a) are NiAl and Ni_3Al, respectively, as verified by EDS analysis. The porosity of the black part is caused by the expansion of trapped air during the melting process. Microcracks are caused by rapid solidification, which occurs through intensive heat transfer to the substrate as it deforms or protrudes from the molten parts that hit the substrate surface at a high speed. In particular, cracks formed at the interface are caused by the difference in coefficients of thermal expansion between the coating material (layer) and the substrate material, and the residual tensile stress generated during cooling. Oxides are formed on the surface of the splats when the molten particles are oxidized and deposited on the substrate. It was confirmed through EDS that the oxide generated at this time was Al_2O_3, as shown by the red cross markers in the surface (c) of **Figure 2**. As shown in **Figure 2**, cross section images of (a) Ni-5Al and (c) Ni-5.5Al-5Mo show a lot of porosity at the interface between the deposition layer and the substrate. But the cross section image of (b) Ni-20Al show a relatively low porosity and cracks, and thus it can be seen that excellent bonding was formed on the substrate to make high-quality contact.

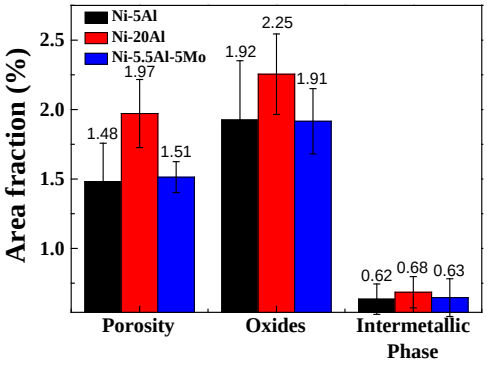

Figure 3: Area fraction of porosity, oxides, and intermetallic phase of (a) surface of Ni-5Al, Ni-20Al, and Ni-5.5Al-5Mo coating

Figure 3 shows the measurement results of the SEM images of the surface and cross-sectional Ni-based coating with oxides and porosity using an image analysis program. The reason that the area fraction of the surface and the cross-section is different is deduced to be that as the Al content increases during the spraying process, the adhesion force of Ni-Al and Ni-Al-Mo particles to the matrix increases relatively, so the porosity area fraction on the surface increases. On the other hand, considering the cross-section, it is believed that a dense coating layer with low porosity was formed by compression during the pass process.

In addition, as the amounts of intermetallic compounds increase, Al dissolves in Ni and becomes more likely to form a solid solution **[15]**, which means they act as the driving force leading to the secondary phase, resulting in an increase in the number of intermetallic compounds as the aluminum content increases. Additionally, as illustrated in **Figure 3**, NiAl and Ni_3Al intermetallic phases are present in Ni-Al and Ni-Al-Mo coatings. These intermetallic compounds are also thermodynamically involved in the bonding strength between the coating layer and the substrate. According to thermodynamic **Equation 1** and **Equation 2** below, an exothermic reaction occurs when the Ni-Al secondary phase is formed. ΔH refers to the heat released during the reaction and depends on the reaction temperature. This is because the exothermic reaction provides a metallic bond between the coating and the substrate [15].

$$Ni + Al \rightarrow NiAl - \Delta H_1 \quad (1)$$

$$3Ni + Al \rightarrow Ni_3Al - \Delta H_2 \quad (2)$$

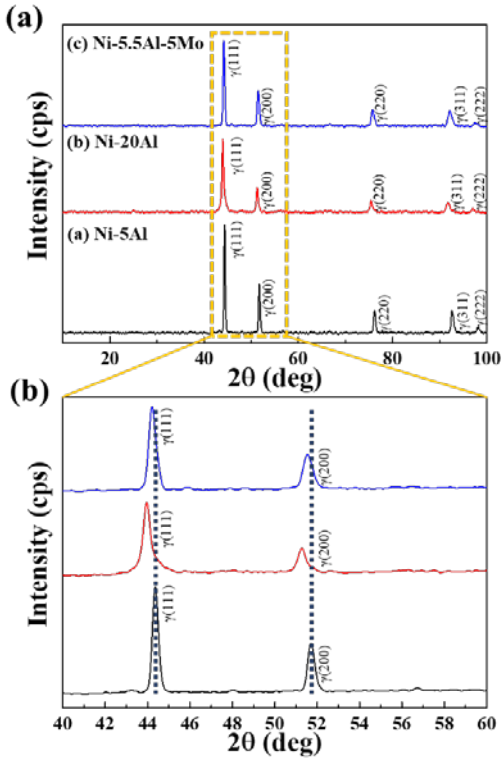

Figure 4: XRD analysis of Ni-5Al, Ni-20Al and Ni-5.5Al-5Mo

3.3 Crystal analysis

The X-ray diffraction values of Ni-5Al, Ni5.5Al-5Mo, and Ni-20Al are shown in **Figure 4**. The detected XRD peaks indicate that as the Al content increases, the widening of the diffraction peaks moves to a lower Bragg angle, which means an increase in the lattice parameters. As shown in **Figure 4**, it is confirmed that FWHM increased as the Al content increased, and it is inferred that the increase in the element content causes fine grains (crystallite), equivalently the grain (crystallite) size decreases. Al and Mo elements cause the diffraction peaks to shift slightly to the left with a small 2-theta value [15]. This is because, according to the Bragg lattice equation (**Equation 3)**, FCC-structured lattice expansion occurs as the interplanar spacing (d) increases leading to a decrease in theta given a constant wave length. When the peak position is shifted left (2 theta smaller), it is interpreted that the d value increases, and when the peak width (full width half maximum) widens, the grain size decreases. It is the change of FWHM that means increase or decrease of grain size. Since the wave length is constant, interplanar spacing (d) increases as theta decreases, that is, it causes FCC-structured lattice expansion, which is caused by a solid solution of Al and Mo, leading to micro-strain in the lattice. In other words, atoms with an atomic radius larger than Ni are dissolved in the matrix, causing FCC

lattice expansion. The atomic radius of Ni, which is a solvent, is 1.24 Å, and the atomic radius of Al and Mo, which are solutes in the Ni matrix, are 1.43 Å and 1.39 Å, respectively.

$$2d\ sin\theta = \mathrm{n}\,\lambda\ (\mathrm{n} = 1,2,3,\cdots) \quad (3)$$

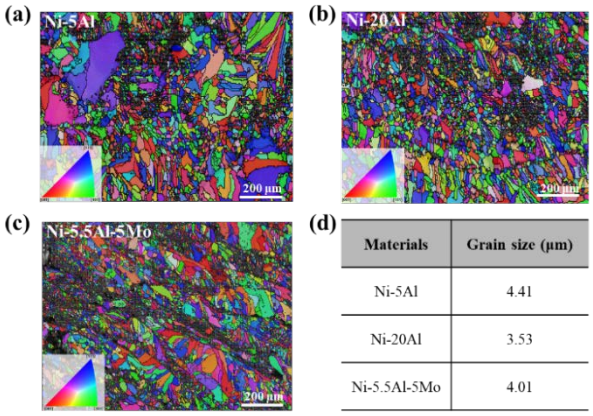

Materials	Grain size (μm)
Ni-5Al	4.41
Ni-20Al	3.53
Ni-5.5Al-5Mo	4.01

Figure 5: IPF images of (a) Ni-5Al, (b) Ni-20Al, (c) Ni-5.5Al-5Mo, and (d) grain size of coating materials

In **Figure 5**, grain size was analyzed using EBSD to confirm the expansion of the FCC lattice structure through XRD. As a result of analyzing using EBSD, the grain size changed with the addition of Al and Mo. **Figure 5** shows that Ni-5Al has a grain size of 4.411 μm, Ni-20Al has a grain size of 3.537 μm, and Ni-5.5Al-5Mo has a grain size of 4.018 μm. The size decreased as the added elements increased, suggesting that an atomic radius of approximately 12% of Ni atom size caused an expansion of the FCC structure. This coincides with the results of changes in the shifted peak and FWHM in the XRD graph in Figure 4, suggesting thath this leads to the refinement of grain size.

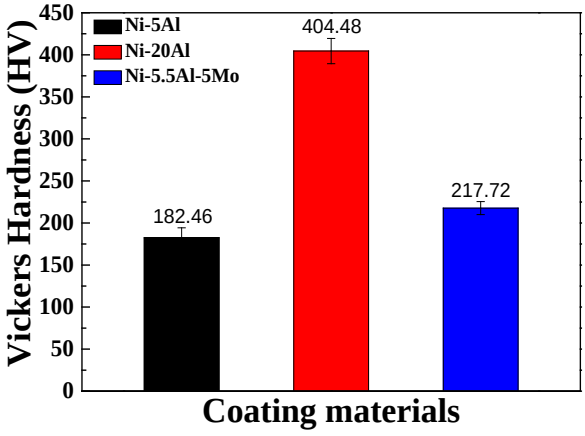

Figure 6: Micro hardness values of the coating layers

3.4 Hardness test

Micro Vickers hardness was analyzed to evaluate the mechanical properties of the coating materials. **Figure 6** shows the results of the micro Vickers hardness test on the coating layer surface according to the Al and Mo contents. The results show that the coating layer of Ni-5.5Al-5Mo was deposited to be thicker than that of Ni-5Al and Ni-20Al. The hardness test results for Ni-5Al in the horizontal direction is 182.46 (± 11.78) HV, for Ni-20Al is 404.48 (± 14.99) HV, and for Ni-5.5Al-5Mo is 217.72 (± 7.78) HV. These mechanical characteristics are consistent with Figure 5, which show the results of the crystallite size (grain size) of each coating layer using EBSD analysis. This suggests that the addition of Al and Mo caused a decrease in grain (crystallite) size and solid-solution strengthening.

4. Conclusions

This study analyzed the microstructure and mechanical characteristics of Ni-based coating due to the addition of Al and Mo based on the measurements of SEM, EDS, XRD and EBSD of the coating layers of Ni-5Al, Ni-5.5Al-5Mo and Ni-20Al in HSLA-100 steels using the twin wire arc spray process. The main results can be summarized as follows. The microstructure of each deposited layer shows a typical lamellar structure of thermal spray coating, and the quantitative amount of intermetallic phase, porosity, and oxides varies depending on the coating materials. The addition of Al and Mo elements causes the expansion of the FCC structure lattice, which promotes the reduction of grain (crystallite) size. The addition of Al and Mo provides changes to the mechanical properties of Ni-based coating. As a result, Ni20Al has the highest values of 404.48 (± 14.99) HV.

Acknowledgement

This work was supported by the Technology development Program(S3249304) funded by the Ministry of SMEs and Startups (MSS, Korea) and the Korea Basic Science Institute (National research Facilities and Equipment Center) grant funded by Ministry of Education (grant No. 2022R1A6C101B738).

Author Contributions

Conceptualization, J. Bang and E. Lee; Methodology, J. Bang; Software, J. Bang; Validation, J. Bang, H. Kwon, E. Byon, and E. Lee; Formal Analysis, J. Bang; Investigation, J. Bang, H. Kwon, E. Byon, and E. Lee; Resources, J. Bang; Data Curation,

J. Bang; Writing—Original Draft, Preparation, J. Bang; Writing—Review & Editing, E. Byon and E. Lee; Visualization, J. Bang; Supervision, E. Lee; Project Administration, E. Lee; Funding Acquisition, E. Lee. All authors have read and agreed to the published version of the manuscript.

References

[1] B. S. Yilbas, I. Toor, and Al-Sharafi, "2.28 anti-corrosive materials, Comprehensive Energy Systems, vol. 2, pp. 913-943, 2018.

[2] H. -K. Park, H. -J. Kim, and C. -G. Park, "Development of preheat-free GMA welding wire for HSLA-100 steel," Journal of Welding and Joining, vol. 29, no. 2, pp. 7-12, 2011 (in Korean).

[3] W. Wu, Q. Wang, L. Yang, *et al.*, "Corrosion and SCC initiation behavior of low-alloy high-strength steels microalloyed with Nb and Sb in a simulated polluted marine atmosphere," Journal of Materials Research and Technology, vol. 9, no. 6, pp. 12976-12995, 2020.

[4] Z. Ahmad, "Chapter 3 - Corrosion kinetics," Principles of Corrosion Engineering and Corrosion Control, pp. 57-119 : Butterworth-Heinemann, 2006.

[5] J. Lee, Y. Jeong, D. Shim, and E. Lee, "Microstructural evolution and martensitic transformation in FeCrV alloy fabricated via additive manufacturing," Materials Science and Engineering: A, vol. 809, 2021.

[6] Y. E. Jeong, J. Y. Lee, E. Lee, and D. Shim "Microstructures and mechanical properties of deposited Fe-8Cr-3V-2Mo-2W on SCM420 substrate using directed energy deposition and effect of post-heat treatment," Materials, vol. 14, no. 5, 2021.

[7] X. Chen, Y. Huang, and Y. Lei "Microstructure and properties of 700 MPa grade HSLA steel during high temperature deformation," Journal of Alloys and Compounds, vol. 631, pp. 225-231, 2015.

[8] E. Byon, "Introduction of ship deck coating method (anti-slip coating and thermal spray coating technology)" Defense & Technology, no. 513, pp. 144-149, 2021 (in Korean).

[9] V. Panwar, V. Chawla, and N. K. Grover, "A review on different thermal spray coating process for industrial applications," International Journal of Latest Trends in Engineering and Technology, Special Issue AFTMME-2017, pp. 064-068, 2017.

[10] G. Yang, Y. Du, S. Chen, Y. Ren, and Y. Ma "Effect of secondary passivation on corrosion behavior and semiconducting properties of passive film of 2205 duplex stainless steel," Journal of Materials Research and Technology, vol. 15, pp. 6828-6840, 2021.

[11] J. Wang, G. Wang, J. Liu, L. Zhang, W. Wang, Z. Li, Q. Wang, and J. Sun "Microstructure of Ni–Al powder and Ni–Al composite coatings prepared by twin-wire arc spraying," International Journal of Minerals, Metallurgy, and Materials, vol. 23, no. 7, pp. 810-818, 2016.

[12] R. Jafari and E. Sadeghi "High-temperature corrosion performance of HVAF-sprayed NiCr, NiAl, and NiCrAlY coatings with alkali sulfate/chloride exposed to ambient air," Corrosion Science, vol. 160, 2019.

[13] G. Moon and E. Lee "Combined effects of optimized heat treatment and nickel coating for the improvement of interfacial bonding in aluminum–iron alloys hybrid structures." Applied Sciences, vol. 11, no. 4, pp. 1-15, 2021.

[14] A. Shabani, S. M. Nahvi, and K. Raeissi, "Effect of heat treatment on structure and oxidation resistance of flame-sprayed Ni-20 wt.% Al on carbon steel," Journal of Thermal Spray Technology, vol. 30, pp. 739-753, 2021.

[15] C. Xu, L. Du, B. Yang, and W. Zhang, "The effect of Al content on the galvanic corrosion behaviour of coupled Ni/graphite and Ni–Al coatings," Corrosion Science, vol. 53, no. 6, pp. 2066-2074, 2011.

[16] E. Kornienko, I. Gulyaev, A. Smirnov, A. Nikulina, A. Ruktuev, V. Kuzmin, and A. Tuezov, "Microstructure and properties of Ni-Al coatings obtained by conventional and high-velocity atmospheric plasma spraying," Results in Surfaces and Interfaces, vol. 6, 100038, 2022.

[17] Y. Wang, Y. Yang, and M. F. Yan "Microstructures, hardness and erosion behavior of thermal sprayed and heat treated NiAl coatings with different ceria," Wear, vol. 263, no. 1-6, pp. 371-378, 2007.

[18] N. P Wasekar, S. Verulkar, M. V. N. Vamsi, and G. Sundararajan, "Influence of molybdenum on the mechanical properties, electrochemical corrosion and wear behavior of electrodeposited Ni-Mo alloy," Surface and Coatings Technology, vol. 370, pp. 298-310, 2019.